Nat. Hazards Earth Syst. Sci., 15, 2449–2459, 2015
www.nat-hazards-earth-syst-sci.net/15/2449/2015/
doi:10.5194/nhess-15-2449-2015

Natural Hazards and Earth System Sciences
Open Access
EGU

Lightning characteristics over the eastern coast of the Mediterranean during different synoptic systems

Y. Ben Ami[1], **O. Altaratz**[1], **Y. Yair**[2,3], **and I. Koren**[1]

[1]Department of Earth and Planetary Sciences, Weizmann Institute of Science, Rehovot, Israel
[2]School of Sustainability, Interdisciplinary Center (IDC), Herzliya, Israel
[3]Department of Life and Natural Sciences, The Open University of Israel, Ra'anana, Israel

Correspondence to: I. Koren (ilan.koren@weizmann.ac.il)

Received: 25 March 2015 – Published in Nat. Hazards Earth Syst. Sci. Discuss.: 10 June 2015
Revised: 16 September 2015 – Accepted: 12 October 2015 – Published: 4 November 2015

Abstract. Thunderstorm activity takes place in the eastern Mediterranean mainly through the boreal fall and winter seasons during synoptic systems of Red Sea Trough (RST), Red Sea Trough that closed a low over the sea (RST-CL), and Cyprus Low (during fall – FCL and winter – WCL). In this work we used the Israeli Lightning Location System ground strokes data set, between October 2004 and December 2010, for studying the properties of lightning strokes and their link to the thermodynamic conditions in each synoptic system.

It is shown that lightning activity dominates over sea during WCL and FCL systems (with maximum values of 1.5 in WCL, and 2.2 km^{-2} day^{-1} in FCL) and have a dominant component over land during the RST and RST-CL days. The stronger instability (high Convective Available Potential Energy (CAPE) values of 762 ± 457 J kg^{-1}) during RST-CL days together with the higher altitude of the clouds' mixed-phase region (3.6 ± 0.3 km), result in a slightly higher density of ground strokes during this system but a lower fraction of positive ground strokes (3 ± 0.5 %). In general the fraction of positive strokes was found to be inversely correlated with the sea surface temperature: it increases from 1.2 % in early fall to 17.7 % in late winter, during FCL and WCL days. This change could be linked to the variation in the charge center's vertical location during those months.

The diurnal cycle in the lightning activity was examined for each synoptic system. During WCL conditions, no preferred times were found through the day, as it relates to the random passage timing of the frontal systems over the study region. During the fall systems (FCL and RST-CL) there is a peak in lightning activity during the morning hours, probably related to the enhanced convection driven by the convergence between the eastern land breeze and the western synoptic winds. The distributions of peak currents in FCL and WCL systems also change from fall to winter and include more strong negative and positive strokes toward the end of the winter.

1 Introduction

Thunderstorms in the eastern Mediterranean (EM) region are associated with three synoptic systems: Cyprus Low (CL), Red Sea Trough (RST), and a hybrid system of Red Sea Trough that closes a low over the sea (RST-CL), (Levin et al., 1996; Altaratz et al., 2003; Ziv et al., 2009). Those storms occur during the boreal fall, winter and early spring (September–April). Throughout summer the area is influenced by the subsidence of the subtropical high that inhibits deep convection.

CL is a mid-latitude low pressure system that is usually generated in the bay of Genoa near the lee side of the Alps (Buzzi and Tibaldi, 1978) and moves eastwards over the Mediterranean Sea (Alpert et al., 1990; Shay-El and Alpert, 1991). The low-level low is accompanied by an upper level trough that transports cold air into the region. According to Shalev et al. (2011) who analyzed lightning activity over the region, more than 71 % of wintertime lightning flashes and 41 % of fall ones occur under this synoptic system. While transported over the Mediterranean, the cold continental air mass is destabilized and its moisture content increases due to the interaction with the warm sea. In proximity to the eastern coast of the Mediterranean Sea, the friction due to the

land–sea interface and the convergence between the western synoptic winds and the eastern land breeze, further aids convection (Heiblum et al., 2011; Ziv and Yair, 1994; Ziv et al., 2009). Under such conditions, thunderclouds develop over the sea, and then are advected into land.

RST is a low-level trough that extends from the African monsoon along the Red Sea towards the EM (Dayan et al., 2001; Kahana et al., 2002). When the upper level trough location enables southern winds in the mid-troposphere, it triggers the transport of tropical moisture towards the EM. Under such conditions, thunderclouds generally develop over the south and eastern part of the EM, exhibiting relatively high cloud bases, $\sim$ 2–3 km above sea level. These conditions occur mainly in fall months (October–November), and are associated with $\sim$ 43 % of the flashes at this time of the year (Shalev et al., 2011). In some cases the RST system extends towards the Mediterranean Sea and forms a close low over the sea, in a complex hybrid situation. Here we refer to this type of system as RST-CL.

Previous works that studied lightning activity over Israel used two types of measuring systems. Levin et al. (1996) investigated the link between the polarity of lightning strokes and the ambient wind conditions using the Tel Aviv CGR3 lightning flash counter. Yair et al. (1998) used the same detection system for examination of the ratio between intracloud (IC) to cloud-to-ground (CG) flashes through the year. Both works were limited to a small domain around the city of Tel-Aviv due to the short detection range of the CGR3 instrument (Mackerras and Darveniza, 1994). Altaratz et al. (2003) and Shalev et al. (2011) surveyed the climatology of ground lightning flashes over a period of several years using data from the national Israel Lightning Location System (ILLS). Altaratz et al. (2003) investigated lightning characteristics over land versus over the sea, while Shalev et al. (2011) discussed the link between the temporal–spatial properties of lightning strokes and the synoptic conditions. They proposed that spatial patterns of lightning strokes can be used as a proxy for the prevailing synoptic condition.

In the present work we study the thermodynamic conditions during specified synoptic systems and their link to the generation of lightning strokes and their properties. We focus on the main synoptic systems that produce electrical activity over the EM: (a) WCL, (b) FCL, (c) RST and (d) RST-CL. So the characteristics of the ground strokes, during these four synoptic systems, are analyzed and linked to the prevailing thermodynamic conditions.

2 Data and methods

2.1 Israel Lightning Location System (ILLS)

The ILLS is composed of eight detectors located in Israel (marked on Fig. 5). The present configuration consists of three types of detectors: five are electric-field-based, two are magnetic field detectors and one is a combined detector that monitors both magnetic and electric fields. The detection algorithm is based on the time of arrival and magnetic field direction techniques (Cummins et al., 1998a, b; Rakov and Uman, 2006) to retrieve information on the peak current intensity, polarity, location and time of impact of ground strokes. The data used in this study were retrieved by the ILLS between October 2004 and December 2010. During the period between 2004 and 2007 only seven detectors were operational. The added detector increased the detection efficiency of the system mainly over the northern edge of the study region. However, due to the big interannual variability in the frequency and location of thunderstorms, we cannot quantify the impact of the improved detection efficiency on our results.

The detection efficiency over Israel, where the point of impact is covered by all detectors, is estimated to be 80–90 % (Yair et al., 2014). The spatial detection accuracy over this region is $\sim$ 500 m and the temporal resolution for detection of successive strokes is $\sim$ 15 µs. The detection efficiency decreases moving away from the network center (Katz and Kalman, 2009). At distances that are larger than 100 km from the Israeli coastline, it is estimated to be only 50 %.

In this study we analyzed strokes data and not flashes. Based on Shalev et al. (2011) findings the multiplicity of CG flashes detected by the ILLS is 1.1 (using thresholds of 1 km and 0.2 s). Therefore we choose to use the raw strokes data as these represent flash data to a good approximation and it do not force the usage of thresholds.

2.1.1 Sensitivity test of detection efficiency

As stated above, the detection efficiency of the ILLS depends on the distance from the center of the network. To reduce errors caused by undetected weak strokes, we investigate the detection efficiency as a function of location and peak current. The focus is on negative strokes because weak positive strokes, with peak currents smaller or equal to 10 kA, are excluded from the data set since they are considered as attributed partly to intra-cloud discharges (Cummins et al., 1998a).

The detection efficiency is estimated here by analyzing the distributions of peak currents as a function of distance from the center of the study region at 32°4′ N and 35° E for days of WCL only. However, similar results are obtained for the other synoptic systems as well.

The distributions for specified narrow peak currents ranges are presented as a function of longitudes (Fig. 1a, c) and latitudes (Fig. 1b, d). Black boxes mark a distance of 250 km from the center of the study region (marked by a black arrow).

Figure 1 shows that small peak current strokes (< 10 kA) are detected only near the center of the study region. This difference is more pronounced in the longitudinal direction. In order to avoid this bias to small currents near the center of

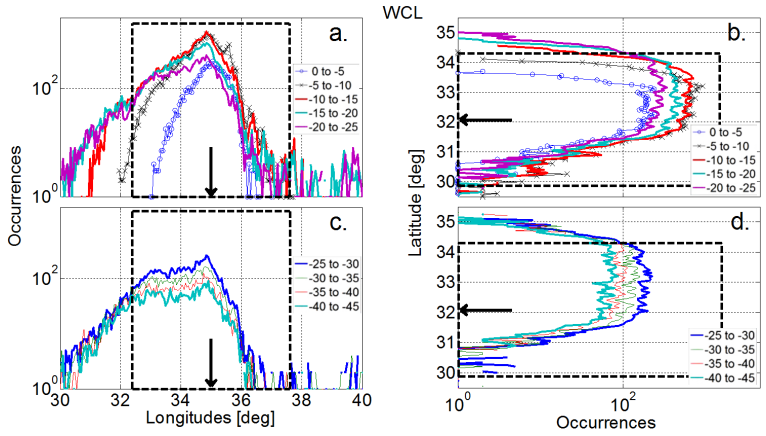

Figure 1. Distribution of peak currents during WCL days. Data are plotted as a function of longitudes (**a** and **c**) and latitudes (**b** and **d**). Distributions are calculated for steps of 5 kA in peak current intensities. (**a** and **b**) are for peak currents between 0 and −25 kA and (**c** and **d**) present the range between −25 and −45 kA. Black boxes mark a distance of 250 km from the center of the study region which is marked by black arrows. Absolute currents larger than 45 kA are not shown.

Table 1. Criteria used for classification of synoptic systems.

Synoptic system	Location of the low'scenter at sea level pressure map		Wind direction at 925 hPa	
	North or west of the Israeli coast	South or southeast of Israel	Northwest to southwest	Northeast to southeast
WCL and FCL	✓	×	×	✓
RST-CL	✓	✓	✓	×
RST	×	✓	×	✓

Israel, we chose to eliminate from the analysis weak negative strokes with peak currents smaller or equal to 10 kA. Note that the preferred occurrence of strokes at lower longitudes and higher latitudes is related to the meteorological (thermodynamic) conditions, a key factor that shapes the spatial distribution of lightning over the region (see Sects. 1 and 3.2.2).

In order to obtain sufficient statistics, on one hand, and to minimize errors due to detection efficiency, on the other hand, the study region is limited to a radius of 250 km. In addition, in order to sharpen the differences between the synoptic systems we filter out days with insignificant electrical activity. Days with fewer than 20 detected strokes are excluded from the data set. The part of the data removed in each synoptic system due to a low number of strokes is less than 0.5 %. Detailed description of the ILLS detection efficiency and location errors is given by Kats and Kalman (2009) and Manoochehrnia et al. (2007).

2.2 Classification of lightning strokes according to the synoptic system

Daily parameters of lightning strokes i.e., peak current intensity (kA) and polarity, location (lat. and long. degree) and time (UTC), are grouped according to the prevailing synoptic conditions and the season. The seasons are defined according to the boreal seasonal distribution: September to November as fall and December to February as winter.

The synoptic conditions (see Table 1) are defined based on examination of daily maps of the Global Data Assimilation System (GDAS, Kanamitsu, 1989). The GDAS data, in spatial resolution of $1° \times 1°$, are provided in 26 pressure levels, between 1000 and 10 hPa (with vertical resolution between 10 and 50 hPa). An additional level is designated for the surface. Data are provided for 00:00, 06:00, 12:00 and 18:00 UTC. Wind direction is examined at 925 hPa and at mean sea level pressure, at 00:00 and 12:00 UTC.

GDAS data are examined with respect to the timing of the detected strokes. Since the formation of thunderstorms over the study region is strongly related to the location and passage of synoptic system, one can follow the location of the synoptic system, via the stroke data. Accordingly, the classification to specific synoptic system is based on examination of the GDAS data at 00:00 or 12:00 UTC combined with the relevant stroke data around this time.

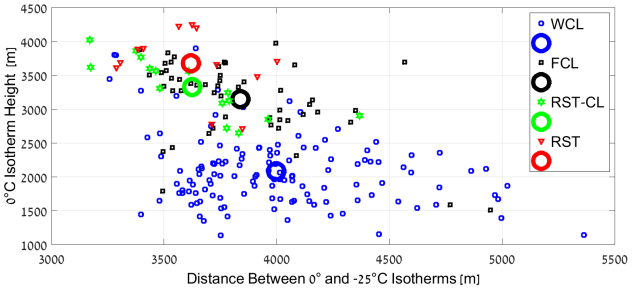

Figure 2. The 0 °C isotherm height above sea level as a function of the depth (thickness) of the atmospheric layer between 0 and −25 °C (m). Results are based on geopotential height of the 0 and −25 °C isotherms using the GDAS database for the area between 32–33° N and 34–35° E. Centroids for the four subsets are marked with circles.

– For specifying CL conditions, the following criteria are used: (a) a center of low pressure at sea level, located north or west of the Israeli coast, (b) northwest to southwest winds at 925 hPa level over the central coast of Israel and (c) the absence of a low pressure system south of Israel.

– For conditions of RST, the criteria are (a) a center of low pressure at sea level located south or southeast of Israel, (b) northeast to southeast winds at 925 hPa and (c) the absence of a dominant low system north or west of the Israeli coast.

– For conditions of RST-CL, the criteria are (a) two distinct centers of low pressure, one located south of Israel and the other one north (or west) of the Israeli coast and (b) western winds in low levels.

Only days that precisely meet the above criteria (see Table 1) are selected for the analysis. Hence the presented analysis does not cover the entire occurrence of lightning in the study region. Table 2 specifies the number and fraction of analyzed days and strokes per synoptic system.

The GDAS data set was also used for determination of thermodynamic conditions during each synoptic system. The height of the 0 and −25 °C isotherms and the Convective Available Potential Energy (CAPE) values were estimated for the area between 32–33° N and 34–35° E as representative values for our study area.

2.3 MODerate resolution Imaging Spectroradiometer (MODIS)

Data from the MODIS instrument onboard the Aqua satellite are used for estimation of sea surface temperature (SST, Kilpatrick et al., 2015). The temperature is estimated for the marine area bounded between 30–34° N and 32–36° E, using the 11 µm band and in spatial resolution of 16 km^2.

Table 2. Number and percentage of days and strokes used in the analysis. The percentages are calculated based on the difference in the data volume after neglecting strokes with absolute peak currents $<=10$ kA, strokes located in radius $>=250$ km from the center of the study region and days when the remaining number of strokes in this radius $<=20$ day^{-1}.

Parameter	WCL	FCL	RST-CL	RST
Number of analyzed days	128	51	15	12
Percent of analyzed days (%)	92.8	87.9	83.3	70.6
Number of analyzed strokes	98963	80861	56994	5118
Percent of analyzed strokes (%)	63.8	70.9	71.5	37.8

3 Results

This section presents characteristics of lightning strokes over the EM analyzed for specified synoptic condition and season. It includes three subsets for the fall season RST, RST-CL and FCL, and one subset for the winter season, WCL. The link to the thermodynamic conditions is examined first.

3.1 Thermodynamic conditions

First the characteristic thermodynamic conditions prevailing during each synoptic system are examined because they determine the properties of thunderclouds (e.g., vertical dimension, updraft speed, water and ice content) and hence the electrical activity.

Figure 2 presents the height and depth (thickness) of the atmospheric layer located between the 0 and −25 °C isotherm levels. In this atmospheric layer resides the mixed-phase region of clouds that is the most relevant to the non-inductive charging mechanism which involves graupel and ice particles and supercooled water (Takahashi, 1978; Saunders et al., 1991; Saunders, 2008). Examination of the vertical location and depth of this atmospheric layer as a function of synoptic condition and season can shed light on the potential for thunderstorms development and lightning production.

During the WCL days the 0 °C isotherm is located around 2 ± 0.5 km (Fig. 2, y axis), much lower than its mean location in the fall synoptic systems, due to the much colder conditions prevailing in the winter. During RST conditions, the location of the 0 °C isotherm is the highest (3.7 ± 0.5 km), and it is 3.3 ± 0.4 km during RST-CL and 3.1 ± 0.5 km during FCL. It means that the mixed-phase region in thunderclouds during the fall season is located higher in the atmosphere, compared to the winter thunderclouds, with the RST thunderclouds located in the highest position within this season (Fig. 2, red centroid).

The depth of this atmospheric layer, between 0 and −25 °C (Fig. 2, x axis) can teach us about the instability of the atmosphere during thunderstorms events. It can be deduced from the thermal lapse rate along this atmospheric layer, where we expect to find the mixed-phase region in thunderclouds. A thinner layer implies more unstable conditions, meaning a

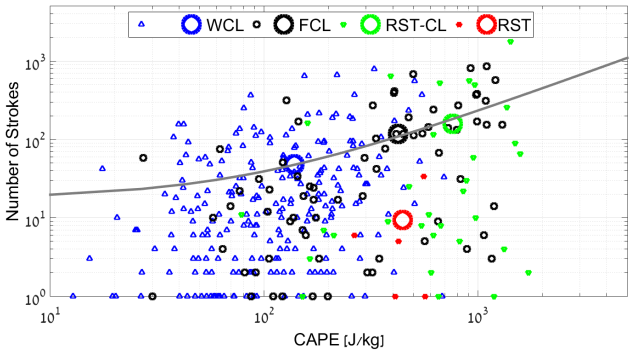

Figure 3. Number of strokes as a function of CAPE according to the four synoptic systems. The CAPE is taken from the GDAS data set. Both variables are estimated for the area between 32–33° N and 34–35° E. The CAPE is estimated at 00:00, 06:00, 12:00 and 18:00 UTC, and the number of strokes is estimated for a time window of ±2 h around these times. Centroids for the four subsets are marked by circles. A linear fit for WCL and FCL and RST-CL is shown in gray.

larger lapse rate (a difference of 25 °C along a shorter distance). A deeper layer, on the other hand, represents smaller instability. During RST conditions this atmospheric layer is the thinnest (3.6 ± 0.2 km); hence it represents the most unstable conditions compared to the other three synoptic systems.

The instability of the atmosphere can be represented by the mean CAPE as well. The CAPE represents the entire atmospheric column and not only the specific layer between 0 and −25 °C as examined in Fig. 2, and it is a commonly used parameter for the characterization of the thermodynamic conditions during thunderstorms. Figure 3 presents the CAPE values per synoptic system as a function of the number of detected strokes. Both variables are estimated for the spatial domain bounded between 32–33° N and 34–35° E. The CAPE is estimated at 00:00, 06:00, 12:00 and 18:00 UTC, and the number of strokes is estimated for a time window of ± 2 hours around these times. Centroids of the four synoptic systems are marked in circles.

The relative position of the mean CAPE values for the four different synoptic systems is quite similar to the one showed in Fig. 2 by the depth of the layer between 0 and −25 °C. Clearly, a trend of general increase in ground strokes production, with the increase in CAPE values, is observed.

The trend is in agreement with many previous studies conducted around the globe (Randell et al., 1994; Williams and Stanfill, 2002) and in Israel (Shalev et al., 2011). WCL, FCL and RST-CL form a positive regression line (marked with gray) between the CAPE values and the number of strokes with regression coefficient $R = 0.41$.

Larger CAPE values (stronger instability) that characterize the synoptic systems of the fall season can better support the required conditions for charge separation within thunderclouds. Those requirements for efficient charging include strong updrafts (Deierling and Petersen, 2008), and enhanced graupel and ice mass fluxes (Deierling et al., 2008). These factors have been shown to be correlated with stronger electrical activity. So the conditions during the RST-CL events create the strongest instability and as a consequence, the best conditions for electrification, as expressed by the daily number of strokes in Fig. 3. During the fall season the temperature of the lower atmosphere and the SST (see Sect. 3.2.4) are still fairly high, therefore the combination with cold air in the upper troposphere creates very unstable conditions (Ziv et al., 2009).

The RST data in Fig. 3 (red circle) are exceptional regarding the fall season systems and are located below the line connecting the other synoptic systems' data. The RST data represent fewer strokes for high values of CAPE, which seems to contradict the previous findings. A possible explanation for this contradiction is higher relative fraction of IC flashes (Yair et al., 1998) that are not detected by the ILLS. The IC flashes can be attributed to the relatively higher-altitude of the mixed-phase region in the clouds during the RST days due to the high-level source of moisture (Kahana et al., 2002; Krichak, et al., 1997; Ziv, 2001). Clouds located higher in the atmosphere, as implied by the higher level of the 0 °C isotherm in Fig. 2, are expected to produce higher ratio of IC to CG flashes (Pierce, 1970; Prentice and Mackerras, 1977; Yair et al., 1998).

It can be noticed that the characteristic CAPE values during fall and winter thunderstorms in Israel are small compared to CAPE values measured around the globe during summer thunderstorms (~ 1000's J kg^{-1}, Williams and Renno, 1993; Williams et al., 2005). The CAPE in our region is similar to other winter thunderstorms like the ones typical for Japan (Suzuki et al., 2011).

Next we examine the characteristics of the lightning strokes and their link to the thermodynamic conditions in more detail.

3.2 Characteristics of lightning strokes

3.2.1 Number of daily strokes as a function of month and synoptic system

Figure 4 shows the monthly averages of number of strokes per day (bars) for the four synoptic systems subsets. The average number of thunderstorm days per month is plotted by red curves. The error bars indicate the interannual variation per month.

The highest electrical activity per thunderstorm-day occurs during October in the RST-CL system (2735 ± 974 day^{-1}). The smallest number of strokes per day is for the FCL system during September. This may be attributed to the very small data set for this month that includes only 1 day with 85 strokes. The interannual variability in the number of strokes per day (indicated by black error bars) is very large

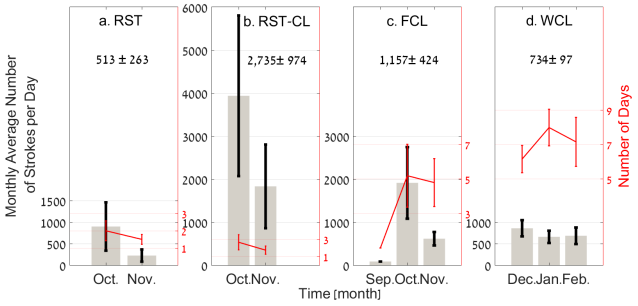

Figure 4. Interannual monthly average number of strokes per day (bar) and the average number of days (red curves) for the four synoptic systems. The error bars indicate standard errors. Seasonal perennial monthly mean and standard error are shown for each system.

for the fall months. It demonstrates the large interannual variability in the magnitude of electrical activity. There are on average only a few days of electrical activity during these months. During winter, on the other hand, the interannual variance is small with a mean value of 734 ± 97 (Fig. 4d).

The level of electrical activity per day, as measured by the number of ground strokes, is highly correlated with the mean value of CAPE per specific synoptic system (Fig. 3). The high flash number during RST-CL systems is supported by the relatively high CAPE values during these time periods and is in agreement with Ziv et al. (2009).

3.2.2 Spatial distribution

The general spatial distribution of lightning strokes detected by the ILLS exhibits a butterfly shape, as is clearly shown in Fig. 5c. This phenomenon is a direct result of the system configuration and the resultant detection efficiency, due to the elongated position of the detectors. The western part of the detection area that spreads mostly over the sea and coastal regions is electrically active during all synoptic systems (Fig. 5a-d). The eastern region that covers a continental area, mainly over eastern Israel, Jordan and Syria, is mostly associated with lightning activity during RST and RST-CL systems.

The average density of strokes ($km^{-2}\,day^{-1}$) in the 250 km radius is 1.1 (WCL), 1.3 (FCL), 1.4 (RST-CL) and 1.1 (RST). Under conditions of WCL, the higher strokes density is detected over the sea and near the coast (Fig. 5a). This location of stronger electrical activity over the sea can be associated with larger instability over the sea (compared to over land) during the winter, as the sea is a source of moisture and heat (Shay-El and Alpert, 1991). In addition, the convergence of the eastern land breeze with the prevailing western synoptic wind near the coast is a key mechanism for enhanced convection and intensification of thunderclouds (Heiblum et al., 2011). During FCL days, the strokes density over the sea is larger than on WCL days and the region of high density is wider. This can be explained by the higher instability during FCL days (higher CAPE, Fig. 3) which enables wide-scale convection over the whole eastern Mediterranean Sea, without the help of convergence near the shore, like in the winter. For the RST and RST-CL days there is high activity both over the sea and over land. During RST conditions the main region of activity is determined by the location of the trough's axis (Zangvil and Druyan, 1990). A western axis, with regard to the coastline, creates substantial activity over the sea and an eastern axis over land. This is the reason for the two separate centers that are shown in Fig. 5d.

3.2.3 Diurnal cycle

The diurnal cycle of lightning activity during different synoptic systems is presented in Fig. 6. It shows substantial differences in the timing of activity between the various systems. For example, the lightning occurrence during RST and FCL synoptic conditions, both during fall, exhibits opposite cycles. In RST conditions, the cycle has two peaks of higher electrical activity, one centered in the afternoon hours (around 17:00 LT), and a second peak in the middle of the night (around 24:00 LT, Fig. 6a). The afternoon peak demonstrates the significance of solar land heating that drives stronger convection.

During FCL, on the other hand, there is one single peak in electrical activity centered in the morning hours, around 09:00 LT (Fig. 6c). The likelihood for lightning activity during late morning hours is $\sim 50\,\%$ higher than in the evening hours. During the RST-CL system (Fig. 6b) the single peak near 06:00 LT is less pronounced and is earlier than the morning peak in the FCL system. During the rest of the time the likelihood is almost constant at $\sim 3\,\%$. This diurnal cycle can be explained by the build-up of the convergence near the coast during the night and early morning, between the synoptic western wind and the eastern land breeze that reaches its maximal magnitude in the early morning hours. During winter, under WCL conditions, the probability is $\sim 4\,\%$ through the entire day, suggesting that the likelihood of electrical activity at any given hour is about equal (Fig. 6d). This could be related to the random timing of the passage of cold fronts over the study region through the day; yet, one can see two minor peaks centered around 06:00 and 22:00 LT. The early morning peak is similar to the one found for the conditions of RST-CL and similar to what was reported by Altaratz et al. (2003) for CL conditions.

3.2.4 Fraction of positive strokes

The relative part of positive strokes, out of total CG strokes, as a function of month and for different synoptic systems, is presented in Fig. 7. Rakov and Uman (2006) discussed a global upper average limit of 10 %. Our results show that under FCL and WCL systems there is a strong increase in the fraction of positive strokes through the months. The fraction

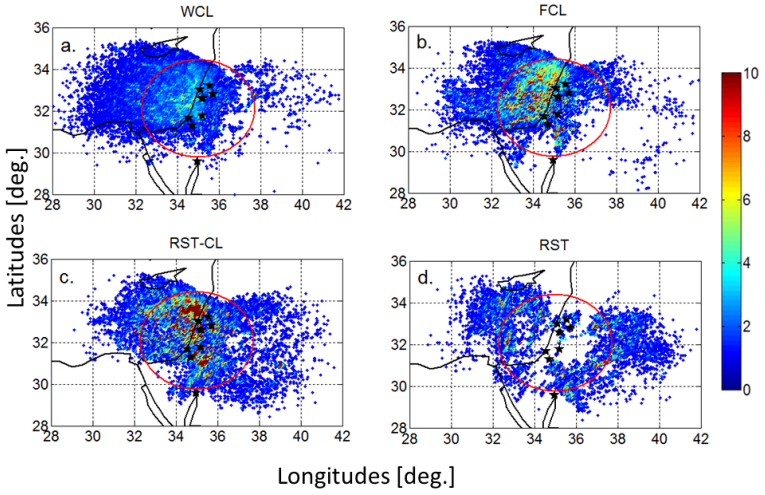

Figure 5. Strokes density according to the four synoptic systems (25 km^{-2} day^{-1}). To highlight spatial features and to compare between all systems, a similar color bar is used (maximum values are 37 in WCL, 54 in FCL, 33 in RST and 131 (25 km^{-2} day^{-1}) in RST-CL). Red circles mark the study region. Black stars mark the location of the ILLS detectors. The average density of strokes in the 250 km radius is 1.1 (WCL), 1.3 (FCL), 1.4 (RST-CL) and 1.1 km^{-2} day^{-1} (RST).

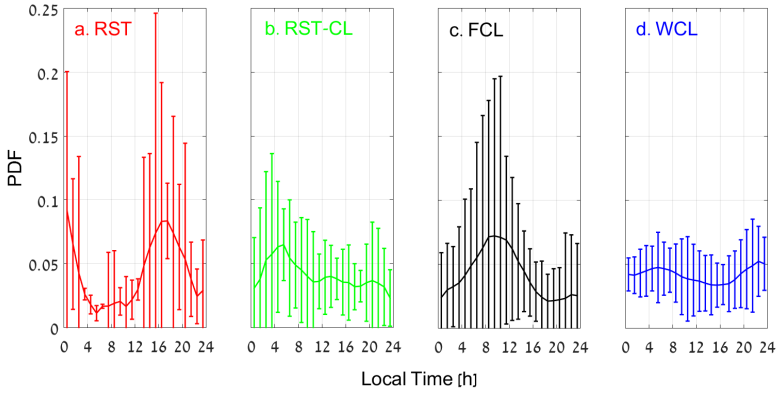

Figure 6. Diurnal probability density function (PDF) of lightning strokes in local time according to the four synoptic systems. The integral under each curve equals 1. Error bars indicate interannual SD.

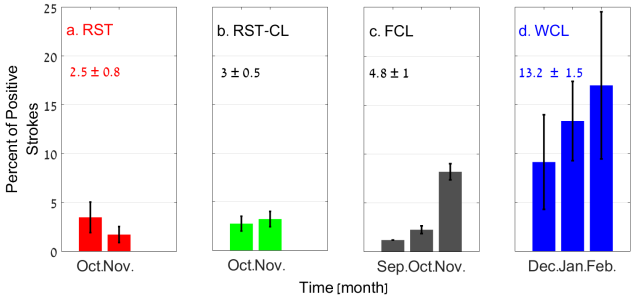

Figure 7. Interannual monthly mean fraction of positive strokes according to the four synoptic systems. The error bars indicate the perennial monthly standard error. Seasonal perennial monthly mean and standard error are shown for each system.

increases from 1.2 ± 1 % in early fall (FCL) to 17 ± 7 % in late winter (WCL). A higher fraction of positive strokes during winter storms was observed in previous studies over this region (Yair et al., 1998) and studies conducted worldwide (e.g., Hojo et al.,1989; Ezcurra et al., 2002; Finke and Hauf, 1996).

This tendency in the fraction of positive strokes emphasizes the impact of the changing thermodynamic conditions on thundercloud properties and hence on the processes of charge separation. Rakov and Uman (2006) reviewed several mechanisms that can explain an increase in the fraction of positive strokes in the cold season. The first mechanism is related to the decrease in the distance between the positive charge center in the cloud and the ground. During winter, due to the decrease in the tropospheric temperatures and in the altitude of the mixed-phase region in clouds (see Fig. 2),

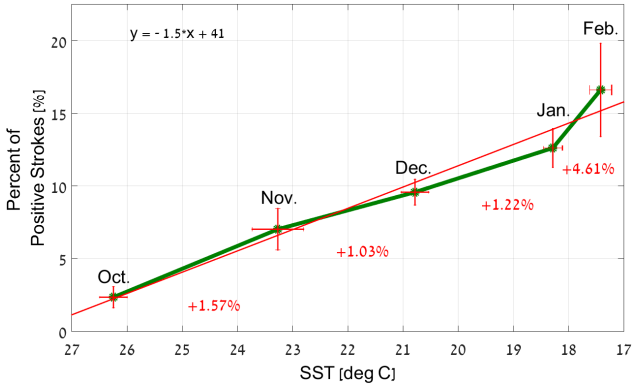

Figure 8. Monthly mean fraction of positive strokes for FCL and WCL systems, between October and February, as a function of the monthly mean SST (green). Note the reverse x axis. Error bars (red) indicate the interannual variations of the two variables. Linear fit is plotted in red. The relative increases in the percent of positive strokes in respect to decrease in the SST are marked by red numbers. SST is calculated based on retrieval from MODIS Aqua, using the 11 µm band for the area between 32–36° E and 30–34° N.

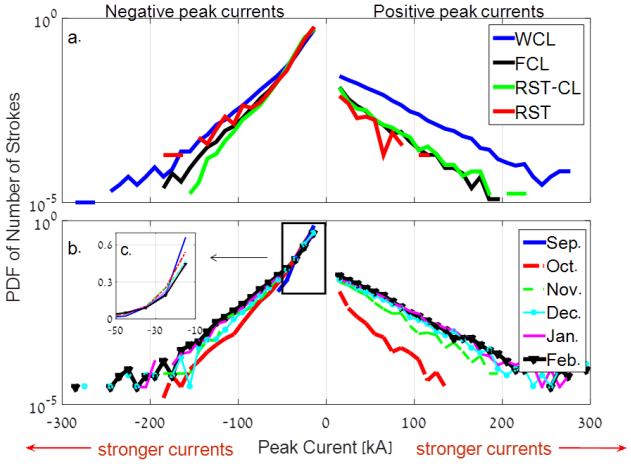

Figure 9. (a) PDF of peak currents (kA) in logarithmic scale as a function of synoptic system. The integral under each curve of positive and negative strokes per synoptic system equals 1; **(b)** monthly PDF for FCL and WCL systems, in logarithmic scale; **(c)** zoom-in window for the area between −35 and −10 kA, marked with a black box on panel **(b)**; it highlights the temporal decrease in fraction of negative weak currents.

the upper positive charge center is closer to the ground. This may increase the probability of positive strokes. An additional proposed mechanism is the better exposure of the upper positive charge center, located near the cloud top and in the anvil, to the ground, due to stronger wind shear in the winter (Brook et al., 1982; Levin et al., 1996; Williams and Yair, 2006). A general trend of an increase in the fraction of positive strokes with the increase in wind shear is found but it could not be quantified with the current GDAS wind data set.

To further explore the dependence of positive strokes' fraction on local thermodynamic factors, we examine its link to the SST. The contribution of SST, as a key factor controlling the thermodynamic conditions of the troposphere, is examined here. Figure 8 shows a strong negative linear correlation ($R = -0.98$) between the monthly SST and the monthly fraction of positive strokes. The dependence shows that for every $\sim 1.5\,^{\circ}$C decrease in SST there is a linear increase of $\sim 1\,\%$ in the fraction of positive strokes (see the linear equation and the red captions in Fig. 8). The colder the sea surface, the larger the fraction of positive ground strokes is. Between January and February we find an exceptional increase of 4.6 %.

This finding supports the suggested mechanism of a higher fraction of positive strokes due to a smaller distance between the upper positive charge center in the cloud and the surface, as discussed above. According to this idea the likelihood for positive strokes increases with decreasing SST due to the derived impact on the temperature of the atmosphere, the smaller vertical development of the cloud and the distance of the positive charge center from the ground (Kitagawa and Michimoto, 1994). Figure 2 indeed indicates that the mixed-phase layer base height is lower by ~ 1–1.5 km during the winter season.

3.2.5 Distributions of peak currents

Figure 9a presents distributions of the peak currents for negative and positive strokes for the four synoptic systems. There are more negative strokes than positive ones under all synoptic systems (Fig. 9a). The median peak current for the negative strokes in all systems is similar, between −18.1 and −20 kA. The positive strokes' distribution has a longer tail, meaning a higher probability for larger peak currents compared to the negative strokes. Therefore their distributions' median values, for the different synoptic systems, are at least 20 % higher than the corresponding absolute negative values.

The larger subsets for FCL and WCL conditions enable us to follow variations in the monthly peak current distributions, from early fall to late winter for conditions of CL. Figure 9b presents the monthly peak current distributions for negative and positive strokes, between September and February. Over time, both the fraction and maximal magnitude of strong currents of both polarities increase. Similar trends have been observed over the east coast of the United States (Orville et al., 1987) and over the Sea of Japan (Hojo et al., 1989). The zoom-in window (Fig. 9c) demonstrates that the increase in strong currents comes simultaneously with a decrease in the fraction of weak negative currents between −35 and −10 kA. The reasons for the increase in magnitude of the strong currents throughout the year are unclear, and will be studied in future work.

4 Discussion and conclusions

The main synoptic systems that produce thunderstorms over the eastern Mediterranean are Red Sea Trough (RST), Red Sea Trough that closed a low over the sea (RST-CL) and Cyprus Low (FCL), all three during fall, and Cyprus Low during the winter (WCL). This study presents the statistical properties of lightning strokes over the eastern Mediterranean (spatial and temporal distribution, diurnal cycle, fraction of positive strokes and distribution of peak currents) as a function of season and synoptic condition, i.e., synoptic systems. These lightning properties are directly related to the thermodynamic conditions prevailing during each system (Ziv et al., 2009).

During RST conditions the source of moisture is in mid-troposphere transport from Africa (Kahana et al., 2002). The thunderclouds are located higher in the atmosphere (the level of the 0 °C isotherm is 3.7 ± 0.5 km) and the atmosphere is very unstable (mean CAPE value of $445 \pm 124\,\mathrm{J\,kg^{-1}}$). The mean number of ground strokes per day is about 15 times lower compared to RST-CL days, while the difference in the CAPE values is minor between those two types of synoptic systems. A possible reason for this difference could be the higher location of the thunderclouds in RST events that could suggest a higher production of IC flashes that are not detected by the ILLS. This assumption is in agreement with Yair et al. (1998) who reported a maximum in the IC to CG ratio in the fall. Under RST conditions, the strokes are distributed mostly over the sea or over land, east and south of Israel but less over the central and northern parts. The main peak of activity is in late afternoon and in the middle of the night. However, there is some uncertainty with these results due to the small data set measured for this synoptic system. The low fraction of positive strokes (2.5 ± 0.8 %) is correlated with the higher location of the mixed-phase part of the thunderclouds in the atmosphere, that leads to a larger distance between the upper positive charge center in the thundercloud and the ground (Rakov and Uman, 2006).

During RST-CL events the mean CAPE values ($762 \pm 457\,\mathrm{J\,kg^{-1}}$) are the highest. The strokes are distributed over the sea and above the entire land area of Israel. There is a peak in thunderstorm electrical activity during early morning hours, correlated with the time of maximal convergence over the sea between the synoptic west wind and the easterly land breeze (Heiblum et al., 2011).

Another type of synoptic system that appears in the fall months is the FCL. This synoptic system is similar to the WCL system as evident from the position of the low pressure in the surface maps. The difference between the two seasons is in the thermodynamic conditions, driving major differences in the properties of thunderclouds and production of their lightning strokes.

During FCL the 0 °C isotherm is located at 3.1 ± 0.6 km, about 1 km higher in the atmosphere than its location in WCL days. The CAPE, $422 \pm 369\,\mathrm{J\,kg^{-1}}$, is about 3 times higher in FCL events and the mean number of strokes per day (117) is about 2.5 times larger. The geographic center of the electrical activity is over the sea during both systems. The diurnal cycle of FCL presents a peak in late morning times, while during WCL there is no major peak, likely due to the arbitrary temporal passage of the cold fronts which is the major driver of the electrical activity.

The trend in the fraction of positive strokes steadily increases from 1.2 ± 1 % in FCL days in September (early fall) to 17 ± 7 % in WCL systems in February (late winter). We note that during CL events (combining both FCL and WCL) the fraction of the positive strokes is inversely correlated with the SST. A colder environment suggests shorter distance between the positive charge centers and the ground. This finding is in agreement with other studies that pointed to a higher fraction of positive strokes in winter storms in Japan (Suzuki, 1992).

The distributions of peak currents in CL conditions also change from fall to winter and include more strong negative and positive strokes toward the end of the winter, with larger median peak currents of positive strokes. This finding is in agreement with observation of lightning properties in winter storms in Japan, where similar conditions occur (Matsui and Hara, 2014).

Overall, the electrical activity over the eastern Mediterranean is somewhat unique with respect to mid-latitude and equatorial regions, as it takes place during fall and winter and not during summertime. It resembles the electrical activity in the Japanese winter in many respects (Williams and Yair, 2006). The winter conditions dictate smaller vertical extent and weaker dynamics.

Further work is needed to better quantify the link between the statistical properties of lightning strokes and the macro/microphysical properties of thunderclouds. Such research has the potential to better quantify the complex relationships between the dynamic and thermodynamic conditions that together determine the nature of the electrical activity of thunderstorms.

Author contributions. The first two authors, Y. Ben Ami and O. Altaratz, contributed equally.

Acknowledgements. We would like to thank K. Lagouvardos and the other anonymous reviewer for their insightful comments. The research leading to these results received funding from the European Research Council (ERC) under the European Union's Seventh Framework Programme (FP7/2007-2013)/ERC grant agreement no. 306965 (CAPRI).

Edited by: G. Panegrossi
Reviewed by: K. Lagouvardos and one anonymous referee

References

Alpert, P., Neeman, B. U., and Shay-El, Y.: Climatological analysis of Mediterranean cyclones using ECMWF data, Tellus A, 42, 65–77, doi:10.1034/j.1600-0870.1990.00007.x, 1990.

Altaratz, O., Levin, Z., Yair, Y., and Ziv, B.: Lightning activity over land and sea on the eastern coast of the Mediterranean, Mon. Weather Rev., 131, 2060–2070, doi:10.1175/1520-0493(2003)131<2060:LAOLAS>2.0.CO;2, 2003.

Brook, M., Nakano, M., Krehbiel, P., and Takeuti, T.: The electrical structures of the Hokuriku winter thunderstorms, J. Geophys. Res., 87, 1207–1215, doi:10.1029/JC087iC02p01207, 1982.

Buzzi, A. and Tibaldi, S.: Cyclogenesis in the lee of the Alps: a case study, Q. J. Roy. Meteor. Soc., 104, 271–287, doi:10.1002/qj.49710444004, 1978.

Cummins, K. L., Murphy, M. J., Bardo, E. A., Hiscox, W. L., Pyle, R. B., and Pifer, A. E.: A combined TOA/MDF technology upgrade of the US National Lighting Detection Network, J. Geophys. Res., 103, 9035–9044, doi:10.1029/98JD00153, 1998a.

Cummins, K. L., Krider, E. P., and Malone, M. D.: The US National Lightning Detection Network™ and applications of cloud-to-ground lightning data by electric power utilities, IEEE T. Electromagn. C., 40, 465–480, doi:10.1109/15.736207, 1998b.

Dayan, U., Ziv, B., Margalit, A., Morin, E., and Sharon, D.: A severe autumn storm over the middle-east: synoptic and mesoscale convection analysis, Theor. Appl. Climatol., 69, 103–122, doi:10.1007/s007040170038, 2001.

Deierling, W. and Petersen, W. A.: Total lightning activity as an indicator of updraft characteristics, J. Geophys. Res., 113, 598, doi:10.1029/2007JD009598, 2008.

Deierling, W., Petersen, W. A., Latham, J., Ellis, S., and Christian, H. J.: The relationship between lightning activity and ice fluxes in thunderstorms, J. Geophys. Res., 113, D15210, doi:10.1029/2007JD009700, 2008.

Ezcurra, A., Areitio, J., and Herrero, I.: Relationships between cloud-to-ground lightning and surface rainfall during 1992–1996 in the Spanish Basque Country area, Atmos. Res., 61, 239–250, doi:10.1016/S0169-8095(01)00133-8, 2002.

Finke, U. and Hauf, T.: The characteristics of lightning occurrence in southern Germany, Contr. Atmos. Phys., 69, 361–374, 1996.

Heiblum, R. H., Koren, I., and Altaratz, O.: Analyzing coastal precipitation using TRMM observations, Atmos. Chem. Phys., 11, 13201–13217, doi:10.5194/acp-11-13201-2011, 2011.

Hojo, J., Ishii, M., Kawamura, T., Suzuki, F., Komuro, H., and Shiogama, M.: Seasonal variation of cloud-to-ground lightning flash characteristics in the coastal area of the Sea of Japan, J. Geophys. Res., 941, 13207–13212, doi:10.1029/JD094iD11p13207, 1989.

Kahana, R., Ziv, B., Enzel, Y., and Dayan, U.: Synoptic climatology of major floods in the Negev Desert, Israel, Int. J. Climatol., 22, 867–822, doi:10.1002/joc.766, 2002.

Kanamitsu, M.: Description of the NMC global data assimilation and forecast system, Weather Forecast., 4, 335–342, doi:10.1175/1520-0434(1989)004<0335:DOTNGD>2.0.CO;2, 1989.

Katz, E. and Kalman, G.: The impact of environmental and geographical conditions on lightning parameters derived from lightning location system in Israel, in: Proceeding of the 10th International Symposium on Lightning Protection, Curitiba, Brazil, November, 9–13 November 2009, 249–254, 2009.

Kilpatrick, K. A., Podestá, G., Walsh, S., Williams, E., Halliwell, V., Szczodrak, M., Brown, O. B., Minnett, P. J., and Evans R.: A decade of sea surface temperature from MODIS, Remote Sens. of Environ., 165, 27–41, doi:10.1016/j.rse.2015.04.023, 2015.

Kitagawa, N. and Michimoto, K.: Meteorological and electrical aspects of winter thunderclouds, J. Geophys. Res., 99, 10713–10721, doi:10.1029/94JD00288, 1994.

Krichak, S. O., Alpert, P., and Krishnamurti, T. N.: Interaction of topography and tropospheric flow – A possible generator for the Red Sea Trough?, Meteorol. Atmos. Phys., 63, 3–4, doi:10.1007/BF01027381, 1997.

Levin, Z., Yair, Y., and Ziv, B.: Positive cloud-to-ground flashes and wind shear in Tel-Aviv thunderstorms, Geophys. Res. Lett., 23, 2231–2234, 1996.

Mackerras, D. and Darveniza, M.: Latitudinal variation of lightning occurrence characteristics, J. Geophys. Res., 99, 10813–10821, doi:10.1029/94JD00018, 1994.

Manoochehrnia, P., Rachidi, F., Rubinstein, M., and Schulz, W.: Lightning Statistics in Switzerland, in: Proceedings of the International Symposium on Lightning Protection, Foz Do Iguassu, Brazil, 26–30 November 2007, 2007.

Matsui, M. and Hara, Y.: The characteristics of winter lightning in Hokkaido as observed by the JLDN, Lightning Protection (ICLP), 2014 International Conference, Shanghai, China, 11–18 October, 116–121, 2014.

Orville, R. E, Weisman, R. A., Pyle, R. B., Henderson, R. W., and Orville Jr., R. E.: Cloud-to-ground lightning flash characteristics from June 1984 through May 1985, J. Geophys. Res., 92, 5640–5644, doi:10.1029/JD092iD05p05640, 1987.

Pierce, E. T.: Latitudinal variation of lightning parameters, J. Appl. Meteorol., 9, 194–195, doi:10.1175/1520-0450(1970)009<0194:LVOLP>2.0.CO;2, 1970.

Prentice, S. A. and Mackerras, D.: The ratio of cloud to cloud-ground lightning flashes in thunderstorms, J. Appl. Meteorol., 16, 545–550, doi:10.1175/1520-0450(1977)016<0545:TROCTC>2.0.CO;2, 1977.

Rakov, V. A. and Uman, M. A.: Lightning: Physics and Effects, Cambridge Univ. Press, Cambridge, UK, 687 pp., 2006.

Randell, S. C., Rutledge, S. A., Farley, R. D., and Helsdon Jr., J. H.: A modeling study on the early electrical development of tropical convection: continental and oceanic (monsoon) storms, Mon. Weather Rev., 122, 1852–1877, doi:10.1175/1520-0493(1994)122<1852:AMSOTE>2.0.CO;2, 1994.

Saunders, C. P. R.: Charge generation and separation charge separation mechanisms in clouds, Saunders, Space Sci. Rev., 137, 335, doi:10.1007/s11214-008-9345-0, 2008.

Saunders, C. P. R., Keith, W. D., and Mitzeva, R. P.: The effect of liquid water on thunderstorm charging, J. Geophys. Res., 96, 11007–11017, doi:10.1029/91JD00970, 1991.

Shalev, S., Saaroni, H., Izsak, T., Yair, Y., and Ziv, B.: The spatio-temporal distribution of lightning over Israel and the neighboring area and its relation to regional synoptic systems, Nat. Hazards Earth Syst. Sci., 11, 2125–2135, doi:10.5194/nhess-11-2125-2011, 2011.

Shay-El, Y. and Alpert, P.: A diagnostic study of winter diabatic heating in the Mediterranean in relation to cyclones, Q. J. Roy. Meteor. Soc., 117, 715–747, doi:10.1002/qj.49711750004, 1991.

Suzuki, T.: Long term observation of winter lightning on Japan Sea Coast, Res. Lett. Atmos. Electr., 12, 53–56, 1992.

Suzuki, T., Matsudo, Y., Asano, T., Hayakawa, M., Michimoto, K.: Meteorological and electrical aspects of several winter thunderstorms with sprites in the Hokuriku area of Japan, J. Geophys. Res., 116, D06205, doi:10.1029/2009JD013358, 2011.

Takahashi, T.: Riming electrification as a charge generation mechanism in thunderstorms, J. Atmos. Sci., 35, 1536–1548, doi:10.1175/1520-0469(1978)035<1536:REAACG>2.0.CO;2, 1978.

Williams, E. and Renno, N.: An analysis of the conditional instability of the Tropical Atmosphere, Mon. Weather Rev., 121, 21–36, doi:10.1175/1520-0493(1993)121<0021:AAOTCI>2.0.CO;2, 1993.

Williams, E. and Stanfill, S.: The physical origin of the land-ocean contrast in lightning activity, C. R. Phys., 3, 1277–1292, doi:10.1016/S1631-0705(02)01407-X, 2002.

Williams, E., Mushtak, V., Rosenfeld, D., Goodman, S., and Boccippio, D.: Thermodynamic conditions favorable to superlative thunderstorm updraft, mixed phase microphysics and lightning flash rate, Atmos. Res., 76, 288–306, doi:10.1016/j.atmosres.2004.11.009, 2005.

Williams, E. R. and Yair, Y.: The microphysical and electrical properties of sprite producing thunderclouds, in: Sprites, Elves and Intense Lightning Discharges, edited by: Füllekrug, M., Mareev, E. A., and Rycroft, M. J., Springer, Dordrecht, the Netherlands, 57–83, 2006.

Yair, Y., Levin, Z., and Altaratz, O.: Lightning phenomenology in the Tel-Aviv area from 1989 to 1996, J. Geophys. Res., 103, 9015–9025, doi:10.1029/98JD00087, 1998.

Yair, Y., Shalev, S., Erlich, Z., Agrachov, A., Katz, E., Saaroni, H., Price, C., and Ziv, B.: Lightning flash multiplicity in eastern Mediterranean thunderstorms, Nat. Hazards Earth Syst. Sci., 14, 165–173, doi:10.5194/nhess-14-165-2014, 2014.

Zangvil, A. and Druyan, P.: Upper air trough axis orientation and the spatial distribution of rainfall over Israel, Int. J. Climatol, 10, 57–62, doi:10.1002/joc.3370100107, 1990.

Ziv, B. and Yair, Y.: The weather in Israel, Unit 5, Hebrew, in: Introduction to Meteorology, The Open University Press, Tel Aviv, Israel, 5–59, 1994.

Ziv, B.: A subtropical rainstorm associated with a tropical plume over Africa and the Middle-East, Theor. Appl. Climatol., 69, 91–102, doi:10.1007/s007040170037, 2001.

Ziv, B., Saaroni, H., Ganot, M., Yair, Y., Baharad, A., and Isaschari, D.: Atmospheric factors governing winter lightning activity in the region of Tel Aviv, Israel, Theor. Appl. Climatol., 95, 301–310, doi:10.1007/s00704-008-0008-6, 2009.